

Published in final edited form as:

J Neurosci Res. 2010 November 1; 88(14): 3161–3170. doi:10.1002/jnr.22472.

Self-assembling peptide amphiphile promotes plasticity of serotonergic fibers following spinal cord injury

Vicki M. Tysseling^{1,*}, Vibhu Sahni^{1,*}, Eugene T. Pashuck², Derin Birch¹, Amy Hebert¹, Catherine Czeisler¹, Samuel I. Stupp², and John A. Kessler¹

¹ Northwestern University's Feinberg School of Medicine, Department of Neurology, Chicago, IL 60611

² Institute for BioNanotechnology in Medicine, Northwestern University, Chicago, IL 60611

Abstract

Injection into the injured spinal cord of peptide amphiphile (PA) molecules that self-assemble and display the laminin epitope IKVAV at high density improved functional recovery after spinal cord injury (SCI) in two different species, rat and mouse, and in two different injury models, contusion and compression. The improvement required the IKVAV epitope and was not observed with the injection of an amphiphile displaying a non-bioactive sequence. To explore the mechanisms underlying these improvements, the number of serotonergic fibers in the lesioned spinal cord was compared in animals receiving the IKVAV-PA, a non-bioactive PA (PA control), or sham injection. Serotonergic fibers were distributed equally in all three groups rostral to the injury, but showed a significantly higher density caudal to the injury site in the IKVAV PA injected group. Further, this difference was not present in the subacute phase following injury but appeared in the chronically injured cord. The IKVAV PA injected groups also trended higher both in the total number neurons adjacent to the lesion and in the number of long propriospinal tract connections from the thoracic to the lumbar cord. IKVAV PA injection did not alter myelin thickness, total axon number caudal to the lesion, axon size distribution, or total axon area. Since serotonin can promote stepping even in complete transection models, the improved function produced by the IKVAV PA treatment may reflect the increased serotonergic innervation caudal to the lesion in addition to the previously demonstrated regeneration of motor and sensory axons through the lesion.

Keywords

spinal cord injury; nanotechnology; biomaterials; regeneration; serotonin

INTRODUCTION

Spinal cord injury (SCI) has devastating effects on motor, sensory, and autonomic function. Even a small amount of neuronal, dendritic, or axonal regeneration could therefore result in life-changing improvements. Although central nervous system (CNS) neurons have the intrinsic ability to regenerate (Richardson, et al., 1980, Schwab and Thoenen, 1985), the environment is non-permissive, and regeneration is limited. However recovery after SCI

Corresponding author: V.M. Tysseling, Northwestern University's Feinberg School of Medicine, 303 East Chicago Avenue, Chicago, Illinois 60611, Telephone: 312.908.5035, Facsimile: 312.503.0872, vmtysse@u.northwestern.edu.

*These authors contributed to this paper equally.

S.S. has founded a company, Nanotope, to eventually develop commercial applications of the self-assembling materials. S.I.S. and J.A.K. participate in this venture.

could result from, local synaptic plasticity or neuroprotection as well as from regeneration. Synaptic rearrangements within the intact lumbar spinal cord below the area of SCI in rodents lead to some restoration of locomotion. Neural circuits within the lumbar spinal cord, termed the central pattern generator (CPG), can produce spontaneous, coordinated, rhythmic alterations of hindlimb flexor and extensor musculature in a walking motion (Barbeau and Rossignol, 1987, Lovely, et al., 1990). Neuromodulators such as serotonin activate and modify the CPG (Schmidt and Jordan, 2000), and serotonin agonists can initiate stepping following complete spinal cord transection (Antri, et al., 2003, Barbeau and Rossignol, 1991, Feraboli-Lohnherr, et al., 1999, Fong, et al., 2005, Guertin, 2004, Guertin, 2004). Transplants of serotonergic neurons or intrathecal serotonin application can also augment locomotor activity (Feraboli-Lohnherr, et al., 1999, Ribotta, et al., 2000). In addition, serotonin has strong facilitatory actions directly on motoneurons themselves (Heckman, et al., 2003, Powers and Binder, 2001).

Locomotor improvement after SCI may also reflect the reconnection of long propriospinal axons which have a documented growth response post SCI (Baldissera, et al., 1981, Bareyre, et al., 2004, Courtine, et al., 2008, Jane, et al., 1964). These axons bridge different spinal segments and can connect intersegmentally. Recovery may also be facilitated by preventing death of neurons and glia. Acute SCI causes necrosis and/or apoptosis contributing to functional deficits (Sekhon and Fehlings, 2001). Loss of oligodendrocytes (OLs) and myelin destroys saltatory conduction and diminishes the function of spared or regenerating axons. The loss of local neurons interrupts spinal circuits and the innervation of the affected spinal segment.

Injection of peptide amphiphile (PA) molecules that self assemble from aqueous solution into cylindrical nanofibers which display the laminin epitope, IKVAV, can facilitate regeneration and improve function in a mouse model of SCI (Tysseling-Mattiace, et al., 2008)(Supplemental Figure 1). These fibers are able to present bioactive sequences at nearly van der Waals density. In this study we sought to determine the anatomical basis of the behavioral improvements resulting from the injection of IKVAV PA. We conclude that major potential contributors to improved behavioral function are an increased density of serotonergic fibers caudal to the lesion and regeneration and/or sparing of motor and sensory axons through the lesion.

MATERIALS AND METHODS

Mouse spinal cord injuries and animal care

All animal procedures were undertaken in accordance with the Public Health Service Policy on Humane Care and Use of Laboratory Animals. The Institutional Animal Care and Use Committee approved all procedures. Adult CD-1 female mice are anesthetized using inhalation anesthetic (2.5% isoflurane in 100% oxygen administered using a VetEquip Rodent anesthesia machine). After laminectomy at the T10 vertebral segment, the spinal cord was compressed dorsoventrally by the extradural application of a 24 g modified aneurysm clip for 1 min (FEJOTA mouse clip). After SCI, the skin was sutured using AUTOCLIP (9 mm; BD Biosciences, San Jose, CA). Mice that exhibited any hindlimb movement 24 h after the injury were excluded from the study. Bladders were manually emptied twice daily. In the event of discomfort, Meloxicam (0.3 mg/kg, s.c. QD) was administered. Gentamycin was administered daily in the event of hematuria (20 mg/kg sc) for 5 d. Neurobehavioral analysis was performed using the Basso, Beattie, and Bresnahan (BBB) scale for the mouse as published for the clip compression model (Joshi and Fehlings, 2002).

Mouse amphiphile injections

PA (1% aqueous solution) was injected 24 h after SCI using borosilicate glass capillary micropipettes (Sutter Instruments, Novato, CA) (outer diameter, 100 μm) coated with Sigmacote (Sigma, St. Louis, MO) to reduce surface tension. The capillaries were loaded onto a Hamilton syringe using a female luer adaptor (World Precision Instruments, Sarasota, FL) controlled by a Micro4 microsyringe pump controller (World Precision Instruments). The amphiphile was diluted 1:1 with a 580 μM solution of glucose just before injection and loaded into the capillary. Under isoflurane anesthesia, autoclips were removed and the injury site was exposed. At 24 hours post injury, the laminectomy is still intact and the bruise created by the lesion is apparent. A stereotaxic Kopf apparatus was used to position the micropipette just dorsal to the lesion. The micropipette was lowered to a depth of 750 μm measured from the dorsal surface of the cord, and 2.5 μl of the diluted amphiphile solution was injected at 1 $\mu\text{l}/\text{min}$. The micropipette was withdrawn at intervals of 250 μm to leave a trail (ventral to dorsal) of IKVAV PA in the cord. At the end of injection, the pipette was left in place for an additional 1 minute, after which it was withdrawn and the wound closed. For all experiments, the experimenters were kept blinded to the identity of the animals.

Rat spinal cord injuries, amphiphile injections and animal care

Adult Long Evans Hooded female rats weighing between 150–200 g were anesthetized using pentobarbital anaesthesia. Laminectomies were performed and the spinal cords contused at spinal segment T13 with a MASCIS impactor (10 gm weight/50mm drop which produces a maximally severe injury). For IKVAV PA injections, 27 gauge needles were used, and the amphiphile was diluted as described above. Twenty-four hours after the contusion injury, rats were re-anesthetized using pentobarbital anaesthesia. Following exposure of the injury site, 5 μl of the diluted amphiphile was injected at 1 $\mu\text{l}/\text{min}$ 0.5 mm rostral and caudal to the lesion epicenter at a depth of 1.5mm. At the end of injection, the needle was left in place for an additional 2 min, after which it was withdrawn and the wound closed. Other animals received a similar injection of the vehicle (glucose solution). In a third group (sham injection), the wound was reopened and then closed without an injection. Rats that exhibited any hindlimb movement 24 h after the injury were excluded from the study. Bladders were manually emptied twice daily. After surgery and in the event of discomfort, (0.5 mg/kg Buprenex BID) was administered. Baytril (2.5mg/kg BID) for 5 days was administered in the event of hematuria. The BBB scale was used for rat neurobehavioral analysis (Basso, et al., 1995).

Animal perfusions and tissue acquisition

Animals were sacrificed using an overdose of carbon dioxide and transcardially perfused with PBS followed by 4% paraformaldehyde in PBS. The spinal cords were dissected and either fixed overnight in 30% sucrose in 4% PFA or fixed for 2 hours in 4% PFA and dehydrated overnight in 30% sucrose. The spinal cords were then frozen in Tissue-Tek O.C.T. embedding compound and sectioned on a Leica (Deerfield, IL) CM3050S cryostat at 20 μm .

Tract tracing and analysis

Mice were anesthetized with Avertin 9 weeks after injury and were injected with mini-ruby-conjugated BDA (Invitrogen) using a 10 μl Hamilton microsyringe fitted with a pulled-glass micropipette. For dorsal column labeling, 2 μl were injected just distal to the L5 dorsal root ganglion. Animals were killed 14 d after BDA injection and perfused. Floating 20 μm sagittal serial sections were each collected and washed three times in 1xPBS and 0.1% Triton X-100, incubated overnight at 4°C with avidin and biotinylated horseradish peroxidase (Vectastain ABC Kit Elite; Vector Laboratories, Burlingame, CA), washed again

three times in 1x PBS, and then reacted with DAB in 50 mM Tris buffer, pH 7.6, 0.024% hydrogen peroxide, and 0.5% nickel chloride. Every section was collected serially so that individual axons could be traced from section to section. Sections were then transferred to PBS and mounted in serial order on microscope slides using a weak mounting media containing 0.1% gelatin and 10% ethanol in PBS. Tracts were imaged using Zeiss (Thornwood, NY) Axiovert fluorescent microscope with the AxioCamHR camera for each axon that was labeled within a 500 μ m distance caudal to the lesion.

Fluorescent Immunohistochemistry

Sections were rinsed with PBS thrice and then incubated with blocking solution (10% normal goat serum (NGS), 0.25% TritonX-100, 1% BSA in PBS) at room temperature for 1 hour. Sections were again rinsed thrice with PBS and incubated with primary antibody (NeuN: 1:500; mouse IgG₁; Chemicon; Serotonin; 1:500; rabbit; Sigma), in blocking solution without NGS at 4 deg C overnight. Sections were then rinsed thrice with PBS and incubated with Alexafluor conjugated secondary antibodies (1:500; Invitrogen, Carlsbad, CA) for 1 h at room temperature. Sections were finally rinsed thrice with PBS and incubated with Hoechst nuclear stain in PBS for 10 minutes at room temperature. After a final rinse with PBS, they were mounted using Prolong Gold anti-fade reagent (Invitrogen) and imaged using a Zeiss (Thornwood, NY) Axiovert fluorescent microscope with an AxioCam HR camera.

Tissue processing for electron microscopy

Animals were sacrificed using an overdose of carbon dioxide and transcardially perfused with PBS followed by 4% paraformaldehyde in PBS. Spinal cords were dissected and fixed overnight in 30% sucrose in 4% PFA. They were then cut along the lesion site and each half was transferred to 0.1M cacodylate buffer overnight. They were then washed in cacodylate buffer thrice and incubated in 2% osmium for one hour and then washed thrice with dH₂O. They were then dehydrated in a series of ethanol washes from 50% to 100% ending in three 10 min in propylene oxide, and subsequently embedded using embedding resin (epon/araldite resin mixture). Each half of the spinal cord was mounted with the lesion side up and sectioned on a Leica Ultramicrotome UC6. Beginning on the lesion side of the spinal cord half, each 1 μ m section was collected, stained with toluidine blue, and imaged on a Zeiss microscope. Once a section was found where all 4 gray matter horns were identifiable, the next section was collected at a thickness of 100 nm, mounted on a 200 mesh copper grid, and stained with uranyl acetate and Reynold's lead citrate each for 10 minutes.

Electron microscope quantification

Images were captured at 2000x on a JEOL 1220 transmission electron microscope. Two non-overlapping images were taken in each dorsal funiculus (one medially and one dorsally) for grids both rostral and caudal to the injury. The axons and myelin were counted and measured using Image J software (NIH)(Supplemental Figure 3). The G ratio was calculated as the diameter of the axon/the diameter of the axon plus myelin (Guy, et al., 1989, Hildebrand and Hahn, 1978).

NeuN counts

Spinal cords were mounted lesion side up on a Leica (Deerfield, IL) CM3050S cryostat and serial sections were mounted on slides. Spinal cord sections were stained with NeuN as above. The quantified cross section was chosen as the first serial cross section outside the lesion that had NeuN staining in all four gray matter horns. Automated multi-channel image acquisition, image stitching, and specimen overview functions of the TissueGnostics software (Vienna, Austria) were used on a Zeiss fluorescent microscope to image the entire

selected cross section for NeuN immunohistochemistry. NeuN+ cells were counted with Image J software (NIH)(Supplemental Figure 3).

Long propriospinal tract analysis

Tracts were labeled by injecting 1 μ l of dextran dye (dextran, Texas Red, 3000 MW, Invitrogen) at 200nl/minute into both the left and right side of the L1 spinal segment. 20 μ m thick cross sections at T9 segment were collected. Five 40X images were taken on the cross section containing labeled neurons; one in each gray matter horn and one centered around the ependyma. Each labeled neuron was counted.

RESULTS

IKVAV-PA injection is beneficial in both rats and mice after contusion or compression SCI

The BBB scale modified for mouse (Basso, et al., 1996, Joshi and Fehlings, 2002) was used to compare the results after SCI of injection of IKVAV-PA versus a non-bioactive (control) PA to assess whether the effects are mediated by the IKVAV sequence. The control PA contains a glutamic acid-glutamine-serine (EQS) head group which has no bioactivity, but can still form nanofibers in a manner similar to IKVAV PA (Silva, et al., 2004). A clip compression model of SCI in mice was used that produces a consistent injury where an initial impact is followed by persistent compression analogous to most cases of human SCI (Joshi and Fehlings, 2002, Joshi and Fehlings, 2002). Parameters were chosen to produce a particularly severe injury. Since a PBS buffer could trigger gelation of the PA before injection, an isotonic glucose solution was used for injections. For this and all subsequent experiments, the experimenters were kept blinded to the identity of the animals. At 24 hours after SCI, the lesion site was injected either with IKVAV PA or the non-bioactive EQS PA, and some animals received sham injection. Injection of IKVAV PA resulted in significant improvement on the BBB scale (8.8) compared to both the EQS PA (7.3) and the sham groups (7.8) (Figure 1a). The IKVAV group (n=16) differs from the EQS (n=14), and sham (n=17) groups at $p < 0.01$ by ANOVA with repeated measures. Tukey Kramer post hoc tests at 10 weeks showed no difference between sham and EQS PA-injected controls, however, the IKVAV PA-injected group differed significantly from the other groups (* $p < 0.05$). The behavioral improvements were comparable to those reported previously even though the strain of mouse used in the two studies differed (129SvJ versus CD-1) (Tysseling-Mattiace, et al., 2008).

To determine whether IKVAV PA injection is similarly beneficial after SCI in other species and using other injury models, the effects of injection were examined in rats subjected to a weight drop contusion injury (Young, 2002). The control used in this experiment was the vehicle for the IKVAV PA, isotonic glucose. The behavioral results from the EQS control and the second most applicable control, vehicle injection, do not differ, therefore we used the vehicle injection in the rat model (Tysseling-Mattiace, et al., 2008). IKVAV PA injection significantly improved behavioral recovery (12.7) compared both to vehicle-injected (9.3) and to sham (8.9) controls (Figure 1b). ANOVA with repeated measures showed that the groups differed from each other ($p < 0.03$). Tukey's HSD post hoc tests showed no difference between sham and vehicle-treated animals at 9 weeks, however, the IKVAV PA-injected group differed from the other groups (* $p < 0.03$). Thus injection of the self-assembling PA resulted in behavioral improvement in two different species (mice and rats), two different strains of mice (129SvJ and CD-1), and two different spinal cord injury models (contusion and compression) (Figure 1)(Tysseling-Mattiace, et al., 2008).

IKVAV PA promotes regeneration of dorsal column sensory axons in CD-1 mice

We previously reported that injection of IKVAV PA promoted both dorsal column and corticospinal tract (CST) regeneration in 129SvJ mice after SCI (Tysseling-Mattiace, et al., 2008). We sought to confirm our previous regeneration results with a different mouse strain, CD-1 by re-examining dorsal column regeneration using tract tracing techniques with BDA. Further, we addressed the need for the IKVAV epitope for the regeneration as noted previously. Sensory rather than motor axon tracing was examined because it is technically easier. We injected BDA into the L5 nerve root, waited 2 weeks for the dye to be transported along the axon, and mounted serial longitudinal sections for tracing of the axons. Representative pictures of sensory axon tracing from IKVAV PA-injected, EQS PA-injected and sham animals at 11 weeks post injury (Figure 2) illustrate the marked difference between the treated and control groups that received BDA injections. Approximately 55% of labeled axons in the IKVAV PA group entered the lesion compared to only about 18% of the fibers in sham controls and less than 10% in EQS PA-injected animals (Figure 2d). Only rare fibers in either control group grew 25% of the way across the lesion, and no fibers in controls penetrated as far as 50%. By contrast, approximately 30% of the fibers in the IKVAV PA-treated group penetrated 25% of the way through the lesion, and about 20% of the fibers penetrated 50% of the distance. Importantly, almost 10% of the fibers actually grew through the lesion and entered the spinal cord rostral to the lesion (Supplemental Figure 2). Most of the fibers followed published criterion for regenerated fibers (Figure 2a) (Steward, et al., 2003). Hence, the IKVAV epitope in the IKVAV PA is essential for the effects on sensory axons after SCI.

IKVAV PA injection increases serotonergic fibers in the caudal spinal cord

Although both these findings and our prior ones (Tysseling-Mattiace, et al., 2008) suggest that injection of IKVAV PA promotes axonal regeneration after SCI, there was insufficient time for fibers to have reached the lumbar spinal cord to reestablish synaptic connections. We therefore sought to determine other mechanisms that could contribute to the functional improvements. Since serotonin can regulate the CPG and facilitate locomotion, we examined the number of serotonin immunoreactive fibers rostral, within, and caudal to the lesion in CD-1 mice comparing the IKVAV PA, EQS PA and sham injected groups. At 10 days post injury, there were serotonergic fibers rostral to the lesion site in all three groups but very few fibers present caudal to the lesion, although the number of fibers in the IKVAV-injected group (13.58) trended slightly higher than EQS (2.29) and sham (1.72) groups (Figure 3). However by 11 weeks post injury the IKVAV PA-injected group contained a significantly ($p < 0.01$ by ANOVA) increased number of serotonin fibers caudal to the lesion (24.16) whereas only scarce fibers were present in the sham (1.73) and EQS (1.15) groups (Figure 4).

Long propriospinal connections trend higher after IKVAV PA injection

Electron microscopy was used to determine whether IKVAV PA injection resulted in significant changes in the overall number of axons caudal to the lesion. There was no difference amongst groups in total axon numbers, mean axon diameter, or the ratio of small (less than 1 μm) to larger axons (more than 1 μm) (Figure 5a–c, k–m). This suggested that the regenerating axons that were described earlier represent a very small subset of the total axons in the dorsal funiculus.

To determine whether plasticity of another subset of axons, the long propriospinal tracts, contributed to improved hindlimb function post SCI as demonstrated in recent studies (Courtine, et al., 2008), dye was injected caudal to the lesion at 4 weeks post injury and labeled neurons rostral to the lesion at around spinal segment T9 were counted 5 weeks post

injury. Although the number of labeled neurons in the IKVAV PA injected group trended higher than the control groups, there were no significant differences amongst the groups.

IKVAV PA injection does not increase myelination in the chronically injured spinal cord

Prior studies have attributed gain of function after some therapeutic interventions to re-myelination in the injured spinal cord (McDonald and Belegu, 2006). We previously reported that injection of IKVAV PA increased the number of CC1+ OLs at 10 days post injury (Tysseling-Mattiace, et al., 2008). We therefore looked five months post injury to determine whether this increase in OLs translated into an increase in stable myelin. Transmission electron microscopy was used to image myelin in the dorsal funiculus just rostral and caudal to the lesion site and myelin thickness was quantitated using G ratio analysis (Guy, et al., 1989, Hildebrand and Hahn, 1978). There were no differences in myelin thickness amongst the three groups suggesting that re-myelination did not contribute to enhanced function in the IKVAV PA group (Figure 5a–c,j).

IKVAV PA injection does not yield a higher number of local neurons

Since IKVAV PA injection attenuates apoptosis adjacent to the lesion 10 days post injury (Tysseling-Mattiace, et al., 2008), we examined the survival of local neurons which might maintain spinal circuitry and increase local function. We examined the number of neurons at 5 weeks post SCI immediately adjacent to the lesion (defined as the point where the four gray matter horns are first observed in cross section, which is a consistent and unbiased way of demarcating the lesion boundary from the adjacent, relatively intact parenchyma. Also, since identifying the exact lesion epicenter is difficult, particularly with cross sections, this provides a reproducible landmark that can be reliably used across animals. As in all experiments, the experimenters were blinded to the identity of the animals. The total number of NeuN+ neurons in the IKVAV group trended higher, however, this was not statistically different from the control groups (Figure 5d–f,n) suggesting that changes in local neuron numbers did not underlie the functional improvements.

In summary, tract tracing again revealed regenerating and/or spared fibers crossing the lesion site only in the IKVAV PA-injected animals and not in the sham-injected or the non-bioactive EQS PA-injected animals. Similarly, serotonin-containing fibers were present caudal to the lesion only in the IKVAV PA-injected group. These findings suggest that the behavioral improvements after injection of IKVAV-PA may reflect cortical input from regenerating and spared tracts and/or from serotonin initiating or modifying the rodent CPG.

DISCUSSION

Consistent behavioral results

An important attribute of a potential therapy for SCI is the consistency of its effects across animal species and in different models of injury, as well as its reproducibility. Since significant variations of injury responses are known to occur in different mouse strains (Basso, et al., 2006, Kigerl, et al., 2006), we studied the effects of IKVAV PA in a variety of different models to determine whether the therapy translates across these differences. In this study we found significant behavioral improvements in two different species (mice and rats), two different strains of mice (129SvJ and CD-1), and two different spinal cord injury models (contusion and compression) (Figure 1) (Tysseling-Mattiace, et al., 2008). Importantly behavioral improvements were not observed after injection of a PA lacking the IKVAV sequence indicating the importance of the sequence for the functional improvement. It is also important to note that the beneficial anatomical changes, when observed, were only observed with the IKVAV PA injection again underlying the necessity for this epitope for the biological effects that were observed. It is noteworthy that we saw significant recovery

much earlier in the CD-1 mouse strain as compared to our previous work with the 129SvJ strain. The behavioral improvements in the CD-1 mice were first apparent within 3 to 4 weeks after SCI, which is much earlier than the observed regeneration with 129SvJ mice and with the rat study, which is too early to be mediated by the regeneration of fibers across the lesion site. This suggested that other mechanisms must also be involved. Some differences between the mouse strains may be related to the effects of injectable anesthesia in the 129SvJ strain, which is less hearty than the CD-1 strain which received an inhalation anesthetic. The rapidity of behavioral recovery in the CD-1 mice may reflect stimulation of the central pattern generator by the increased number of serotonergic fibers. The exact serotonin receptor subtype for central pattern generator modulation has not been clarified fully although 5HT7 has been implicated (Liu, et al., 2009). Notably, the mouse study and the rat study also differed in the level of recovery. We attribute this to the different models used: the MASCIS impactor model in the rat and the clip compression model in the mouse. We have much more consistent results with the clip compression model and the severe injury results in much lower baseline behavioral scores.

IKVAV promotes axonal regeneration and/or sparing following SCI

We previously reported that injection of IKVAV PA promoted both dorsal column sensory and corticospinal (CST) motor fiber regeneration in 129SvJ mice after SCI (Tysseling-Mattiace, et al., 2008). In this study we performed tract tracing of dorsal column sensory axons in a different mouse strain, CD-1, and again found fibers traversing the lesion site only in the IKVAV PA injected group. In both this study and in our past work, 10% of labeled dorsal column fibers consistently grew through the lesion. A small subset of fibers in this study could be followed completely through the section which was approximately 2 spinal segments. Since this subset of fibers was notably longer than the others in this study as well as those seen in our previous study, some fiber sparing in the CD-1 mouse strain cannot be ruled out. When we quantified axon number, axon diameter, and small:large axon ratios in the entire dorsal funiculus rostral and caudal to the injury site we found no differences amongst the three groups (Figure 5). This is not surprising since the relatively small number of regenerating dorsal column fibers would not be expected to significantly impact the overall number of axons in such a study. This further highlights the necessity of tracing individually labeled fibers for the regeneration analysis. Prior studies suggest that small changes in fibers can lead to a significant behavioral difference (Basso, 2000), and our studies are consistent with this view. However the relatively early recovery of function caused by the IKVAV PA in CD-1 mice suggested that mechanisms other than the axon regeneration must also be involved in this process.

IKVAV PA promotes sublesional neuroplasticity

IKVAV PA injection significantly increased the number of serotonin containing fibers caudal to the lesion. In fact, at 11 weeks post injury serotonin fibers were found caudal to the lesion almost exclusively in the IKVAV-PA group. Previous studies have shown that increased serotonin signaling from embryonic raphe nuclear transplants, serotonergic agonists, or direct application of serotonin produces significant behavioral improvements that are attributed to increased serotonin modulation of the central pattern generator (CPG). (Barbeau and Rossignol, 1991, Feraboli-Lohnherr, et al., 1999, Fong, et al., 2005, Ribotta, et al., 2000, Schmidt and Jordan, 2000). This suggests that the behavioral improvements after IKVAV-PA injection reflected, at least in part, the increased density of serotonin-containing fibers in the caudal spinal cord. Effects of serotonin on motoneurons are also well known, but in complete spinal injury, motoneurons undergo a plastic recovery in response to loss of serotonin and thereby regain high levels of excitability (Bennett, et al., 2001, Li and Bennett, 2003). Thus, the post-injury effects on the CPG may be more important than a direct effect on the motoneurons caudal to the lesion site. We cannot determine from our data whether

these are descending serotonin fibers that regenerated across the lesion site or local sprouting/upregulation of fibers although sublesional sprouting seems most likely.

In our previous study we found that the regeneration of the sensory and motor fibers occurred between 2 weeks and 11 weeks post injury (Tysseling-Mattiace, et al., 2008), and this study showed a comparable timeline for the serotonin regeneration/sprouting (Figure 3–4). Since the stability of the nanofibers in the spinal cord is on the order of weeks (Tysseling-Mattiace, et al., 2008), it seems likely that the regeneration and/or sprouting occurred after the degradation of the material. In fact the timing of the degradation of the IKVAV PA may be important for its success in facilitating growth of fibers through the lesion site. Permanent grafts using Schwann cells or other non-biodegradable materials can effectively promote axonal growth into, but not through, the transplanted material or tissue because regenerating axons will not exit the favorable microenvironment of the graft (Bunge, 2001). By contrast degradation of the IKVAV PA after ingrowth of axons may have allowed regenerating axons to continue to grow past the lesion site.

IKVAV PA injection does not affect chronic myelination or local neuron number

Although our prior study demonstrated that injection of IKVAV-PA increases the number of oligodendrocytes at and adjacent to the lesion site, this study did not find any differences in unmyelinated fibers (data not shown) or in myelin thickness amongst the three groups (Figure 5). The increase in oligodendrocyte number, which was observed at an acute stage of the injury, thus did not lead to a long term change in myelination and is unlikely to account for the behavioral improvements. Interestingly, despite evidence from other studies that remyelination may be vital to recovery, in this study very few demyelinated fibers were found 5 months post injury (data not shown) and myelin thickness averaged higher than expected (Figure 5) (Guy, et al., 1989, Hildebrand and Hahn, 1978). Most groups that have investigated demyelination and remyelination following injury have looked in the subacute and not chronic stages of SCI (Keirstead, et al., 2005, Liu, et al., 2000, McDonald and Belegu, 2006), and a recent study by Lasiene et al posits that chronic demyelination does not exist after SCI in mice (Lasiene, et al., 2008). Our observations are consistent with the findings of that study.

Since IKVAV PA injection also attenuated the number of apoptotic cells surrounding the lesion at 10 days post injury (Tysseling-Mattiace, et al., 2008), we were interested in determining whether this decrease in apoptosis resulted in increased numbers of local neurons and thus possibly more local controls and/or intact spinal circuitry. However no differences in neuron numbers were found in cross sections adjacent to the lesion suggesting that the changes in apoptosis did not reflect altered neuronal survival.

Overall, we conclude that injection of IKVAV-PA into the injured spinal cord consistently improves behavioral outcome. The major potential contributors to the improved behavioral function produced by IKVAV PA treatment are the presence of serotonin caudal to the lesion as well as the previously demonstrated and now confirmed regeneration of axons through the lesion.

Supplementary Material

Refer to Web version on PubMed Central for supplementary material.

Acknowledgments

PI Stupp(Kessler) Regenerative Scaffold Technologies for CNS and Diabetes NIH/National Institute of Biomedical Imaging and Bioengineering 5 R01EB003806-05

Thanks to Northwestern University's Cell Imaging Facility with their imaging assistance. Special thanks are given to Lennell Reynolds for the electron microscopy tissue processing. Thanks to Mike Pizzi for the NeuN counts. This study was supported by a grant from the Byron Riesch Foundation, by NIH R01 NS20778 and by a scholarship from the Foundation for Physical Therapy.

References

1. Antri M, Mouffle C, Orsal D, Barthe JY. 5-HT_{1A} receptors are involved in short- and long-term processes responsible for 5-HT-induced locomotor function recovery in chronic spinal rat. *Eur J Neurosci*. 2003; 18:1963–1972. [PubMed: 14622228]
2. Baldissera, F.; Hultborn, H.; Illert, M. Integration in spinal neuronal systems. In: Brooks, V., editor. *Handbook of Physiology. The Nervous System. Motor Control*. American Physiological Society; Bethesda: 1981. p. 509-595.
3. Barbeau H, Rossignol S. Recovery of locomotion after chronic spinalization in the adult cat. *Brain Res*. 1987; 412:84–95. [PubMed: 3607464]
4. Barbeau H, Rossignol S. Initiation and modulation of the locomotor pattern in the adult chronic spinal cat by noradrenergic, serotonergic and dopaminergic drugs. *Brain Res*. 1991; 546:250–260. [PubMed: 2070262]
5. Bareyre FM, Kerschensteiner M, Raineteau O, Mettenleiter TC, Weinmann O, Schwab ME. The injured spinal cord spontaneously forms a new intraspinal circuit in adult rats. *Nat Neurosci*. 2004; 7:269–277. [PubMed: 14966523]
6. Basso DM, Beattie MS, Bresnahan JC. A sensitive and reliable locomotor rating scale for open field testing in rats. *J Neurotrauma*. 1995; 12:1–21. [PubMed: 7783230]
7. Basso DM, Beattie MS, Bresnahan JC, Anderson DK, Faden AI, Gruner JA, Holford TR, Hsu CY, Noble LJ, Nockels R, Perot PL, Salzman SK, Young W. MASCIS evaluation of open field locomotor scores: effects of experience and teamwork on reliability. Multicenter Animal Spinal Cord Injury Study. *J Neurotrauma*. 1996; 13:343–359. [PubMed: 8863191]
8. Basso DM, Fisher LC, Anderson AJ, Jakeman LB, McTigue DM, Popovich PG. Basso Mouse Scale for locomotion detects differences in recovery after spinal cord injury in five common mouse strains. *J Neurotrauma*. 2006; 23:635–659. [PubMed: 16689667]
9. Bennett DJ, Li Y, Siu M. Plateau potentials in sacrocaudal motoneurons of chronic spinal rats, recorded in vitro. *J Neurophysiol*. 2001; 86:1955–1971. [PubMed: 11600653]
10. Bunge MB. Bridging areas of injury in the spinal cord. *Neuroscientist*. 2001; 7:325–339. [PubMed: 11488398]
11. Courtine G, Song B, Roy RR, Zhong H, Herrmann JE, Ao Y, Qi J, Edgerton VR, Sofroniew MV. Recovery of supraspinal control of stepping via indirect propriospinal relay connections after spinal cord injury. *Nat Med*. 2008; 14:69–74. [PubMed: 18157143]
12. Feraboli-Lohnherr D, Barthe JY, Orsal D. Serotonin-induced activation of the network for locomotion in adult spinal rats. *J Neurosci Res*. 1999; 55:87–98. [PubMed: 9890437]
13. Fong AJ, Cai LL, Otoshi CK, Reinkensmeyer DJ, Burdick JW, Roy RR, Edgerton VR. Spinal cord-transected mice learn to step in response to quipazine treatment and robotic training. *J Neurosci*. 2005; 25:11738–11747. [PubMed: 16354932]
14. Guertin PA. Role of NMDA receptor activation in serotonin agonist-induced air-stepping in paraplegic mice. *Spinal Cord*. 2004; 42:185–190. [PubMed: 14758350]
15. Guertin PA. Synergistic activation of the central pattern generator for locomotion by l-beta-3,4-dihydroxyphenylalanine and quipazine in adult paraplegic mice. *Neurosci Lett*. 2004; 358:71–74. [PubMed: 15026151]
16. Guy J, Ellis EA, Kelley K, Hope GM. Spectra of G ratio, myelin sheath thickness, and axon and fiber diameter in the guinea pig optic nerve. *J Comp Neurol*. 1989; 287:446–454. [PubMed: 2794129]
17. Heckman CJ, Lee RH, Brownstone RM. Hyperexcitable dendrites in motoneurons and their neuromodulatory control during motor behavior. *Trends Neurosci*. 2003; 26:688–695. [PubMed: 14624854]
18. Hildebrand C, Hahn R. Relation between myelin sheath thickness and axon size in spinal cord white matter of some vertebrate species. *J Neurol Sci*. 1978; 38:421–434. [PubMed: 310448]

19. Jane JA, Evans JP, Fisher LE. An Investigation Concerning the Restitution of Motor Function Following Injury to the Spinal Cord. *J Neurosurg.* 1964; 21:167–171. [PubMed: 14127616]
20. Joshi M, Fehlings MG. Development and characterization of a novel, graded model of clip compressive spinal cord injury in the mouse: Part 1. Clip design, behavioral outcomes, and histopathology. *J Neurotrauma.* 2002; 19:175–190. [PubMed: 11893021]
21. Joshi M, Fehlings MG. Development and characterization of a novel, graded model of clip compressive spinal cord injury in the mouse: Part 2. Quantitative neuroanatomical assessment and analysis of the relationships between axonal tracts, residual tissue, and locomotor recovery. *J Neurotrauma.* 2002; 19:191–203. [PubMed: 11893022]
22. Keirstead HS, Nistor G, Bernal G, Totoiu M, Cloutier F, Sharp K, Steward O. Human embryonic stem cell-derived oligodendrocyte progenitor cell transplants remyelinate and restore locomotion after spinal cord injury. *J Neurosci.* 2005; 25:4694–4705. [PubMed: 15888645]
23. Kigerl KA, McGaughy VM, Popovich PG. Comparative analysis of lesion development and intraspinal inflammation in four strains of mice following spinal contusion injury. *J Comp Neurol.* 2006; 494:578–594. [PubMed: 16374800]
24. Lasiene J, Shupe L, Perlmutter S, Horner P. No evidence for chronic demyelination in spared axons after spinal cord injury in a mouse. *J Neurosci.* 2008; 28:3887–3896. [PubMed: 18400887]
25. Li Y, Bennett DJ. Persistent sodium and calcium currents cause plateau potentials in motoneurons of chronic spinal rats. *J Neurophysiol.* 2003; 90:857–869. [PubMed: 12724367]
26. Liu J, Akay T, Hedlund PB, Pearson KG, Jordan LM. Spinal 5-HT7 receptors are critical for alternating activity during locomotion: in vitro neonatal and in vivo adult studies using 5-HT7 receptor knockout mice. *J Neurophysiol.* 2009; 102:337–348. [PubMed: 19458153]
27. Liu S, Qu Y, Stewart TJ, Howard MJ, Chakraborty S, Holekamp TF, McDonald JW. Embryonic stem cells differentiate into oligodendrocytes and myelinate in culture and after spinal cord transplantation. *Proc Natl Acad Sci U S A.* 2000; 97:6126–6131. [PubMed: 10823956]
28. Lovely RG, Gregor RJ, Roy RR, Edgerton VR. Weight-bearing hindlimb stepping in treadmill-exercised adult spinal cats. *Brain Res.* 1990; 514:206–218. [PubMed: 2357538]
29. McDonald JW, Belegu V. Demyelination and remyelination after spinal cord injury. *J Neurotrauma.* 2006; 23:345–359. [PubMed: 16629621]
30. Powers RK, Binder MD. Input-output functions of mammalian motoneurons. *Rev Physiol Biochem Pharmacol.* 2001; 143:137–263. [PubMed: 11428264]
31. Ribotta MG, Provencher J, Feraboli-Lohnherr D, Rossignol S, Privat A, Orsal D. Activation of locomotion in adult chronic spinal rats is achieved by transplantation of embryonic raphe cells reinnervating a precise lumbar level. *J Neurosci.* 2000; 20:5144–5152. [PubMed: 10864971]
32. Richardson PM, McGuinness UM, Aguayo AJ. Axons from CNS neurons regenerate into PNS grafts. *Nature.* 1980; 284:264–265. [PubMed: 7360259]
33. Schmidt BJ, Jordan LM. The role of serotonin in reflex modulation and locomotor rhythm production in the mammalian spinal cord. *Brain Res Bull.* 2000; 53:689–710. [PubMed: 11165804]
34. Schwab ME, Thoenen H. Dissociated neurons regenerate into sciatic but not optic nerve explants in culture irrespective of neurotrophic factors. *J Neurosci.* 1985; 5:2415–2423. [PubMed: 4032004]
35. Sekhon LH, Fehlings MG. Epidemiology, demographics, and pathophysiology of acute spinal cord injury. *Spine.* 2001; 26:S2–12. [PubMed: 11805601]
36. Silva GA, Czeisler C, Niece KL, Beniash E, Harrington DA, Kessler JA, Stupp SI. Selective differentiation of neural progenitor cells by high-epitope density nanofibers. *Science.* 2004; 303:1352–1355. [PubMed: 14739465]
37. Steward O, Zheng B, Tessier-Lavigne M. False resurrections: distinguishing regenerated from spared axons in the injured central nervous system. *J Comp Neurol.* 2003; 459:1–8. [PubMed: 12629662]
38. Tysseling-Mattiace VM, Sahni V, Niece KL, Birch D, Czeisler C, Fehlings MG, Stupp SI, Kessler JA. Self-assembling nanofibers inhibit glial scar formation and promote axon elongation after spinal cord injury. *J Neurosci.* 2008; 28:3814–3823. [PubMed: 18385339]

39. Young W. Spinal cord contusion models. *Prog Brain Res.* 2002; 137:231–255. [PubMed: 12440371]

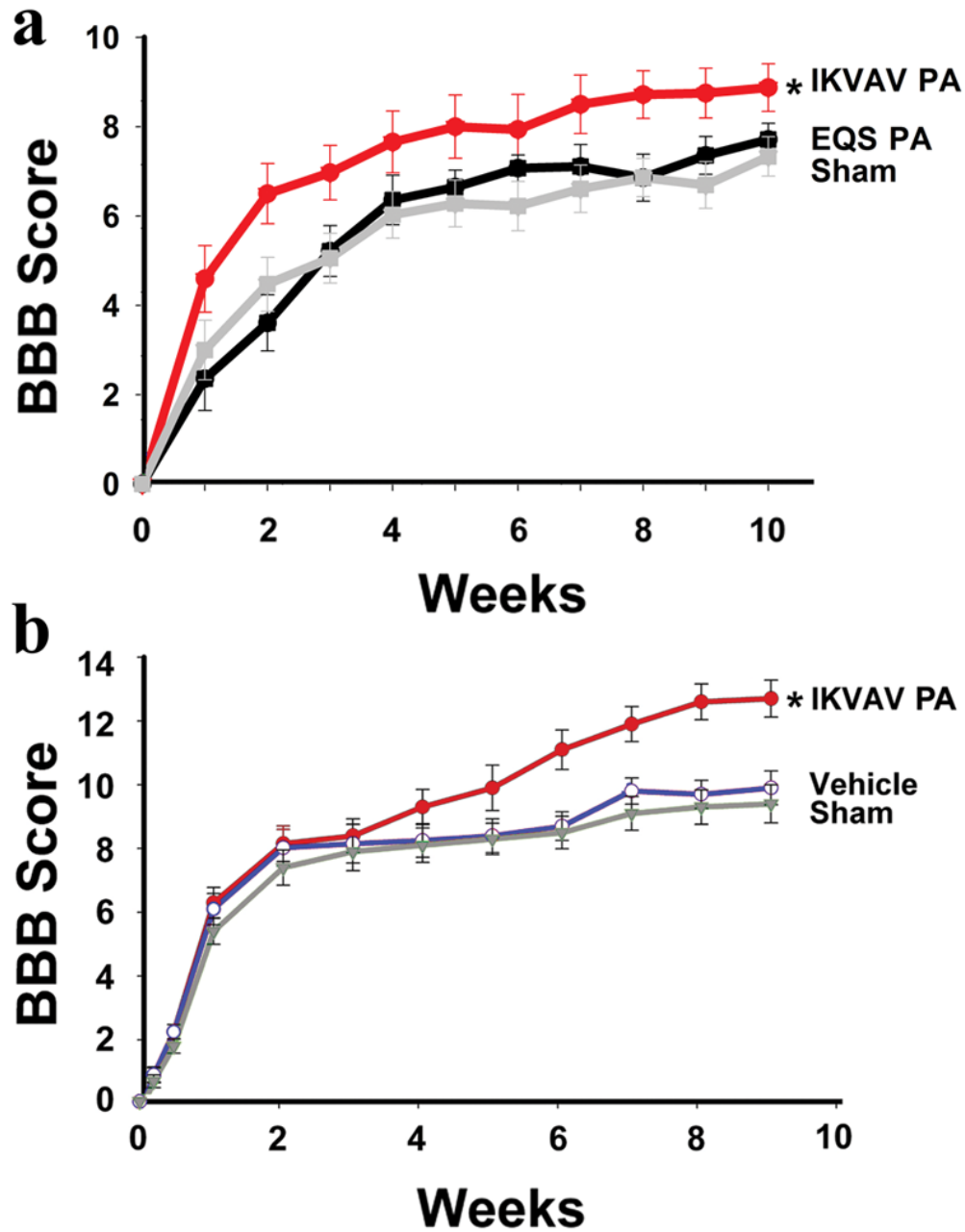


Figure 1. IKVAV PA promotes functional recovery as analyzed by the BBB scale
A, Graph showing mean mouse BBB locomotor scores after severe compression SCI. The IKVAV (n=16), EQS (n=14), and sham (n=17) groups differ from each other at $p < 0.01$ by ANOVA with repeated measures. Tukey Kramer post hoc t tests showed no difference between sham and EQS PA-injected controls, however, the IKVAV PA-injected group differed significantly from the other groups at 10 weeks ($*p < 0.05$). **B**, Graph showing mean rat BBB locomotor scores after moderately severe contusion SCI. ANOVA with repeated measures showed that the groups differed from each other ($p < 0.03$). Tukey's HSD post hoc t tests showed no difference between sham and vehicle-treated animals, however, the IKVAV PA-injected group differed from the other groups at 9 weeks ($*p < 0.03$).

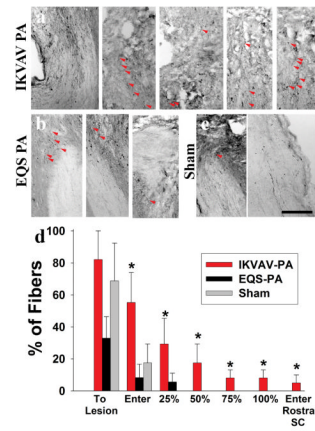


Figure 2. IKVAV PA promotes regeneration of sensory axons after SCI

A–C, Red arrows on bright-field images of BDA-labeled tracts show fibers through the lesion only in the IKVAV PA-injected group (**A**), but just up to and slightly into lesion in EQS PA-injected (**B**) and sham (**C**). Bar graphs show the extent to which labeled dorsal column axons penetrated the lesion. $p < .006$ by the Kruskal-Wallis rank test. Scale bar: 100 μm .

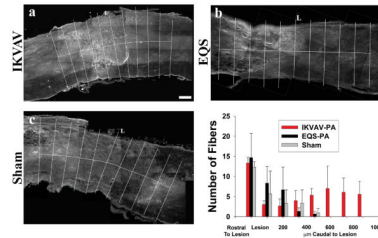


Figure 3. Similar numbers of serotonin fiber numbers rostral and caudal to lesion at 10 days post SCI

A–C, Representative monochrome pictures of serotonin staining around the lesion in IKVAV PA-injected (A), EQS-injected (B), or sham (C). D, Bar graph shows that there are more fibers rostral to the injury than caudal at 10 days post SCI, but no difference between the IKVAV PA-injected, EQS-injected, or sham groups either rostral or caudal to the lesion. Scale bar: 200 μ m.

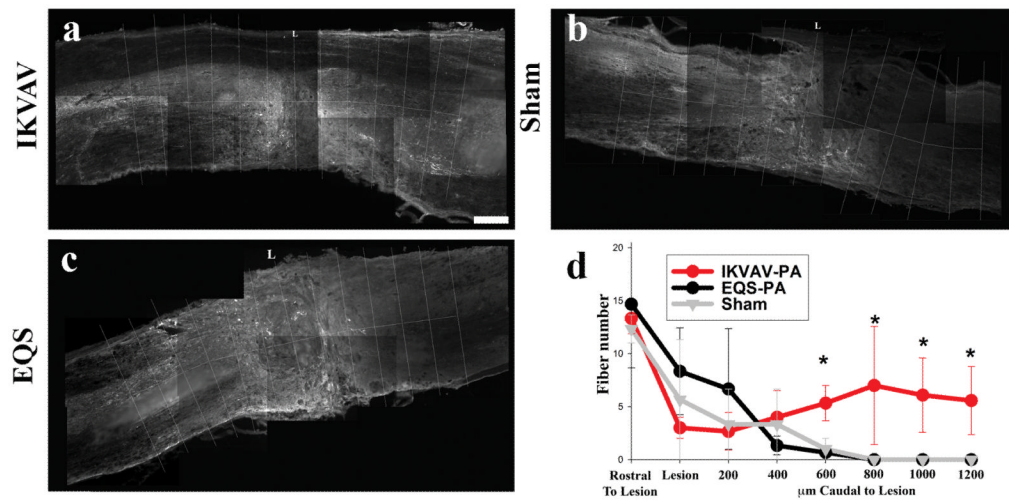


Figure 4. Serotonin fibers are only caudal to lesion in IKVAV PA-injected animals
A–C, Representative monochrome pictures of serotonin staining around the lesion in IKVAV PA-injected (**A**), EQS-injected (**B**), or sham (**C**). **D**, Bar graph shows similar numbers of serotonin fibers rostral to lesion, however, the IKVAV-PA had significantly more serotonin fibers from 600 μm caudal to the lesion as shown by ANOVA ($p < 0.006$). Note that serotonin-containing fibers are virtually only found in the IKVAV PA-injected group 800 μm and more caudal to the lesion epicenter (**A,D**). Scale bar: 200 μm .

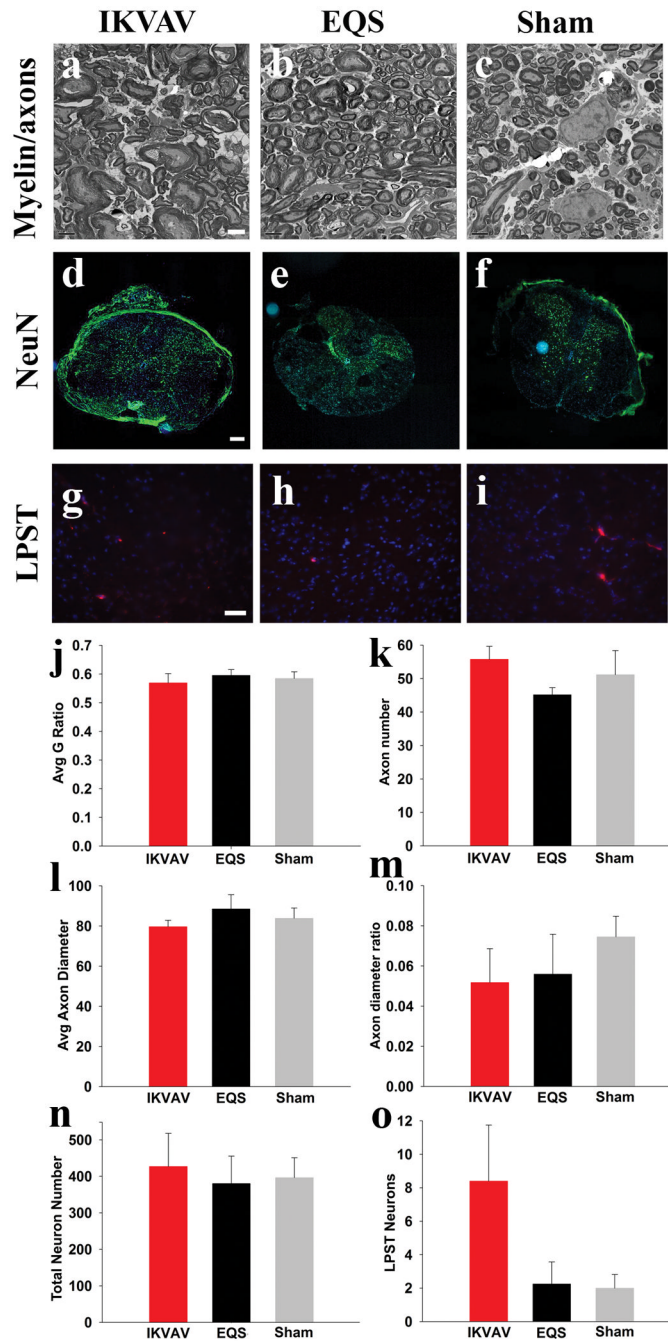


Figure 5. Changes in myelin thickness, axon diameter, axon number, neuron number, and long propriospinal tracts did not contribute to behavioral improvements
A–C, Representative electron microscope images of IKVAV PA, EQS PA, and sham groups from which the myelin and axon data were derived. Scale bar: 2 μ m. **D–F**, Representative fluorescent microscope images of neurons in spinal cord cross sections. (blue: Hoechst, green: NeuN) Scale bar: 200 μ m. **G–I**, Representative fluorescent microscope images of long propriospinal tract (LPST) labeled neurons. (blue: Hoechst, red: rhodamine dye for LPST neurons). Scale bar: 20 μ m. **J–O**, Bar graphs showing no significance between all groups for myelin G ratio (J), total axon number (K), mean axon diameter (L), ratio of

small:large diameter axons (M), total neurons near lesion (N), or long propriospinal tract connections (O).